Potent neutralization of severe acute respiratory syndrome (SARS) coronavirus by a human mAb to S1 protein that blocks receptor association

Jianhua Sui*, Wenhui Li†, Akikazu Murakami*, Azaibi Tamin‡, Leslie J. Matthews*, Swee Kee Wong†, Michael J. Moore†, Aimee St. Clair Tallarico*, Mobolaji Olurinde*, Hyeryun Choe§, Larry J. Anderson‡, William J. Bellini‡, Michael Farzan†, and Wayne A. Marasco*¶

*Department of Cancer Immunology and AIDS, Dana–Farber Cancer Institute; §Perlmutter Laboratory, Pulmonary Division, Children's Hospital, Department of Pediatrics, and †Partners AIDS Research Center, Brigham and Women's Hospital, Department of Microbiology and Molecular Genetics, Department of Medicine, Harvard Medical School, Boston, MA 02115; and ‡National Center for Infectious Diseases, Centers for Disease Control and Prevention, Atlanta, GA 30333

Effective prophylaxis and antiviral therapies are urgently needed in the event of reemergence of the highly contagious and often fatal severe acute respiratory syndrome (SARS) coronavirus (SARS-CoV) infection. We have identified eight recombinant human single-chain variable region fragments (scFvs) against the S1 domain of spike (S) protein of the SARS-CoV from two nonimmune human antibody libraries. One scFv 80R efficiently neutralized SARS-CoV and inhibited syncytia formation between cells expressing the S protein and those expressing the SARS-CoV receptor angiotensin-converting enzyme 2 (ACE2). Mapping of the 80R epitope showed it is located within the N-terminal 261–672 amino acids of S protein and is not glycosylation-dependent. 80R scFv competed with soluble ACE2 for association with the S1 domain and bound S1 with high affinity (equilibrium dissociation constant, $K_d = 32.3$ nM). A human IgG1 form of 80R bound S1 with a 20-fold higher affinity of 1.59 nM comparable to that of ACE2 ($K_d = 1.70$ nM), and neutralized virus 20-fold more efficiently than the 80R scFv. These data suggest that the 80R human monoclonal antibody may be a useful viral entry inhibitor for the emergency prophylaxis and treatment of SARS, and that the ACE2-binding site of S1 could be an attractive target for subunit vaccine and drug development.

T he severe acute respiratory syndrome (SARS)-associated coronavirus (SARS-CoV), a newly emergent member in the family Coronaviridae, causes SARS for which there are no vaccines or effective therapies currently available (1–4). It has been reported that high titers of protecting IgG antibody to SARS-CoV are present in convalescent serum, and SARS patients show clinical improvement if they are given serum from previously infected patients (5, 6). These observations suggest that passive immunization with human monoclonal antibodies could be developed for the treatment of SARS (7). The spike (S) proteins of coronaviruses are large type-I transmembrane glycoproteins that are responsible for receptor binding and membrane fusion. Two functional domains at the amino (S1) and carboxy (S2) termini of the S protein are conserved among the coronaviruses. The S1 and S2 domain of SARS-CoV S protein can be identified by sequence alignment with other coronavirus S proteins, especially with the more conserved S2 domain (8–10). The S protein is also the major antigenic determinant for coronaviruses (9, 11–14). It has recently been demonstrated that the binding of the S1 domain to its receptor angiotensin-converting enzyme 2 (ACE2) on host cells is responsible for SARS-CoV entry into cells (15). Therefore, we targeted the S1 protein for generation of neutralizing human monoclonal antibodies. Here we report the identification, production, and characterization of a neutralizing human monoclonal antibody 80R against SARS-CoV that blocks the binding of S1 to ACE2.

Materials and Methods

Expression and Purification of SARS-CoV S1 and Truncated S1.
Plasmids encoding SARS-CoV S protein residues 12-672, 12-327, or 261-672 fused with the constant region fragment of human IgG1 [named as S1-Ig, S1 (327)-Ig and S1 (261-672)-Ig, respectively] were transfected into 293T cells for transient expression. A plasmid encoding residues 12-672 of S protein fused C-terminally with C9 (S1-C9) was also transfected into 293T cells for expression. The Ig-tagged proteins were purified by protein A Sepharose. Anti-C9 antibody 1D4 obtained from the National Cell Culture Center was conjugated with protein A Sepharose and used for purification of S1-C9. The purity was detected by SDS/PAGE, and the protein concentration was determined by a protein assay kit (Bio-Rad).

Selection of Phage Library and Screening of Phage Antibodies.
Two human nonimmune single-chain variable region fragment (scFv) libraries (a total of 2.7×10^{10} members) constructed from B cells of 57 unimmunized donors were used for selection of scFvs against the purified S1-C9. Plaque-forming units (5×10^{11}) of phage-scFvs prepared from each library were mixed and introduced for panning into Maxisorp immunotubes (Nunc) coated with 10 μg of S1-C9. Nonspecifically absorbed phages were removed by intensive washings. Specific bound phages were eluted with 100 mM triethylamine, neutralized, amplified, and used for further selections as described (16). Randomly picked single phage-scFv clones were screened for specific binding to S1-C9 by ELISA after three rounds of panning. Briefly, 96-well Maxisorp immunoplates were coated with 0.2 μg of S1-C9 per well or control proteins HIV-1 gp120-C9 and BSA, blocked with PBS containing 4% nonfat milk. Phage-scFvs in PBS containing 2% nonfat milk were added. Specific bound phages were detected by adding horseradish-peroxidase-conjugated mouse anti-M13, and the system was developed by adding TMB substrate. Absorbance at 450 nm was measured. Clones that bound to S1-C9 with A_{450} values of >1.0 were scored as positive, whereas negative clones gave values of <0.2. For S1-C9 specific binding clones, the genes of variable regions of heavy (VH) and light (VL) chain were sequenced, and their corresponding amino acid sequences were aligned.

Expression and Purification of scFvs and Whole Human IgG1.
The VH and VL gene fragments of S1-specific scFvs were cloned into

---

prokaryotic expressing vectors. Some of them were cloned into pSyn1 vector (17, 18), expressed in *Escherichia coli* XL1-Blue (Stratagene), and purified from the periplasmic fractions. The others were cloned into pET22b(+) vector (Novagen), expressed in *E. coli* BL21(DE3) (Novagen), and purified from insoluble fraction of the inclusion bodies. All scFvs contain a His-6 tag that allows purification by immobilized metal affinity chromatography. The scFvs purified from the periplasmic extracts were dialyzed in PBS, and the scFvs purified from inclusion bodies were renatured by dialyzing in 0.4 M L-arginine containing buffer followed by PBS. The S1-binding activity of purified soluble scFvs was confirmed by ELISA by using S1-C9 and S1-Ig. The rabbit anti-His-6 polyclonal antibody (Santa Cruz Biotechnology) and horseradish peroxidase-labeled anti-rabbit Ig (Pierce) were used to detect the bound scFvs in ELISA. For production of whole human IgG1, the VH and VL gene fragments of scFv were separately subcloned into human IgG1κ expression vector TCAE5 (19). IgG1 was expressed in 293T cells by transient transfection and purified by protein A Sepharose affinity chromatography.

Microneutralization Assay. To preserially diluted antibody samples in 96-well tissue culture plates, $\approx$37 plaque-forming units of SARS-CoV (Urbani strain) were added, and the mixture was incubated at 37°C for 1 h. Subsequently, $\approx$2 $\times$ 10^5 Vero E6 cells were added to each antibody/virus mixture, and the plate was incubated further at 37°C/5% CO_2 for 3–4 days. To visualize the results, the plate was stained with crystal violet-formaldehyde stain (0.013% crystal violet, 2.5% ethanol, and 10% formaldehyde in 0.01 M PBS) for 1 h at room temperature. The endpoint of the microneutralization assay was defined as the dilution at which >50% of the testing wells are not protected from infection; in the other words, the endpoint titer is reached when three or two of three wells are not protected. The assay was performed in triplicate.

Syncytia Inhibition Assay with Anti-S1 Antibodies. 293T cells, $\approx$30% confluent in T75 flask, were transfected with plasmids encoding a codon-optimized form of full length of SARS-CoV S protein or receptor ACE2. One day after transfection, cells were trypsinized and washed once in medium. Those S protein-expressing cells were premixed with 0, 25, 50, and 100 nM of anti-S1 scFvs or IgG1 for 10 min at room temperature, mixed with cells expressing ACE2 at a 1:1 ratio, and plated on 24-well plates. Cells were cultured in the presence of antibodies. After 36 h, syncytia were observed, and representative photographs were taken.

Affinity Measurement by Biacore. The binding kinetics and affinity of neutralizing antibody and receptor ACE2 to the purified S1-Ig were analyzed by surface plasmon resonance (Biacore 3000, Uppsala, Sweden). The purified S1-Ig was covalently immobilized to a CM5 sensor chip via amine group using the amine coupling kit (Biacore) in 10 mM sodium acetate buffer, pH 4.5. Experiments were run at a flow rate of 10 μl/min in HBS-EP buffer (Biacore). The surface was regenerated with 10 mM glycine-HCl, pH 2.0. Binding kinetic parameters were measured with antibodies or receptor at different molar concentrations and evaluated with BIA-EVALUATION software (Biacore).

Flow Cytometry Analysis of Inhibition of S1 Binding to Vero E6 Cells by Antibody. scFvs (0, 5, 15, or 30 μg/ml) were mixed with 15 μg/ml S1-Ig in a 40-μl volume at 4°C for 1 h. Each mixture was added to Vero E6 cells (2 $\times$ 10^5) and incubated at 4°C for 1 h. S1 (327)-Ig was used as S1-Ig control also incubated with Vero E6 cells. Cells were washed three times with PBS containing 0.5% BSA and 0.1% NaN$_3$. For detection of S1-Ig binding to Vero E6 cells, FITC-labeled goat anti-human IgG (Pierce) was

used as secondary antibody and incubated with cells at 4°C for 30 min. Cells were washed as above. Samples were analyzed by using FACScan with CELLQUEST software (both from Becton Dickinson).

Radioimmunoprecipitation Assay of Inhibition of S1 Binding to Soluble ACE2 by Antibody. S1-Ig (1.5 μg) was mixed with different amounts (0.1, 0.5, 1.5, 4.5 μg) of scFvs and incubated at 4°C for 1 h. Soluble ACE2 was expressed in 293T cells and metabolically labeled for 24 h with [^{35}S]cysteine and [^{35}S]methionine (NEN Life Science). The premixed S1-Ig and scFvs or goat anti-human ACE2 polyclonal antibody (R & D Systems) were added to 100 μl of metabolically labeled ACE2 and protein A Sepharose beads and incubated for 1 h at 4°C. The beads were washed four times with PBS containing 0.25% NP$_{40}$ and 0.01% SDS. Bound proteins were eluted in reducing Laemmli sample buffer at 100°C for 5 min. Proteins were separated by 8% SDS/PAGE and visualized by autoradiography on Kodak Biomax MR film.

Deglycosylation of S1-Ig and Western Blotting with scFv. The purified S1-Ig was deglycosylated with PNGase F (New England Biolabs), an enzyme that removes N-linked glycosylation, under denaturing conditions according to the manufacturer's instructions. For Western blotting, 50 ng of S1-Ig, S1 (327)-Ig, S1 (261–672)-Ig, or deglycosylated S1-Ig were reduced by boiling in 20 μl of reducing sample buffer (50 mM DTT/1% SDS), or 50 ng of S1-Ig was denatured in denaturing sample buffer (1% SDS). Those samples were subjected to 10% SDS/PAGE. The S1 and truncations of S1 were blotted by anti-S1 scFv and followed by polyclonal rabbit anti-His-6 antibody (Santa Cruz Biotechnology) and then horseradish peroxidase-labeled anti-rabbit IgG (Pierce). The luminometric detection was performed by using the SuperSignal Chemiluminescent substrate kit (Pierce).

Results and Discussion

Identification of Anti-S1 Phage Antibodies, Expression, and Purification of Soluble scFvs. Purified recombinant S1-C9 was used as antigen to select antibodies from two nonimmune human scFv libraries. After three rounds of selection on S1-C9, a total of 288 clones were screened for S1 specific binding by ELISA. One hundred four clones specifically recognized S1-C9 protein but not HIV-1 gp120-C9 and BSA control proteins. Eight unique anti-S1 scFvs were identified (6A, 8C, 12E, 26H, 27D, 80R, 91M, and 92N) by sequencing analysis of the individual clones (Table 1). Eight different VH and seven different VL sequences were revealed (one scFv 6A did not contain a VL). The gene families were VH1 and VH3 for VH and Vλ1, Vλ2, Vλ8, Vκ1, and Vκ3 for VLs. Further, the eight scFvs tagged with His-6 were expressed in *E. coli* and purified by immobilized metal affinity chromatography. Vector pSyn1 was used for expression of the 6A, 80R, 91M, and 92N, and vector pET22b(+) was used for the other four scFvs expression because of their lower expression level in pSyn1. The binding activity and specificity of the scFvs were confirmed by ELISA with S1-C9 and S1-Ig.

Neutralizing Activity of 80R and Affinity of 80R and ACE2. Neutralizing activity of the purified soluble anti-S1 scFvs for SARS CoV (Urbani strain) was tested on susceptible Vero E6 cells by a microneutralization assay. One of eight scFvs, 80R (VH3/Vκ3), showed neutralization activity (Fig. 1*A*). The finding that monovalent scFv 80R has potent neutralizing activity *in vitro* demonstrated that SARS-CoV neutralization does not require bivalent binding. However, the very fast blood clearance of monovalent scFv fragments represents a major limitation for their utilization in passive immunotherapy. In most cases, the bivalent full-length immunoglobulin is more effective than their corresponding scFv because of avidity effects, effector functions, and prolonged serum half-life. Therefore, 80R scFv was converted to a bivalent

Table 1. Amino acid sequence of anti-S1 scFvs

VH

	1 FW1	CDR1	FW2	CDR2	FW3	CDR3	FW4	Family
Consensus	QVQLVQSGGG.V.PG.SLRLSCAASGFTFS	SY.MS	WVRQAPGKGLEWV.	.IS..GS..YYADSVKG	RFTISRDNSKNTLYLQMNSLRAEDTAVYYCAR	D.............DY	WGQGTLVTVSS	
6A	.........V.Q..R.............V.	.NY..	..............S	V.YSG..T-........	..............................K	.YGEGF----------..	....	V$_H$3
8C	E.........L.K..G.............	.Y..	.I..........S	Y..SS..TI........	..............G......	.WGYSFG---------.-	....	V$_H$3
12E	.......AEVKK..A.VKV..K...Y..T	T.GI.	.......Q....MG	W..AYNGNTN..QKLQ.	.V.MTT.T.TS.A.MELR...SD.........	VGYYYGDYAWGYYYYGM.V	....	V$_H$1
26H	....QE....L.K..G.............	D.Y..	.I..........S	Y..SS..TI........	.........A..S........	ERWLQIGEDAF-----.I	.....T......	V$_H$3
27D	.........LIQ..G.............V.	.NY..	..............S	V.YSG..T-........		NFGEDF----------..	....	V$_H$3
80R	E.........V.Q..K...........A..	..A.H	.............A	V..YD..NK........		.RSYYL----------..	....	V$_H$3
91M	.........L.Q..G..............	.SW..	.............A	Y.KQD..EK..V.....	.........A..S.....D..........	.QGWGWDGTEYYS---..	....	V$_H$3
92N	.......AEVKK..A.VKV..K...Y..T	S.GI.	.......Q....MG	W..AYNGNTN..QKLQ.	.V.MTT.T.TS.A.MELR...SD.........	.DLSDYGEWLGP----..	....	V$_H$1

VL

	137 FW1	CDR1	FW2	CDR2	FW3	CDR3	FW4	Family
Consensus	Q..LTQP.S.SGSPGQR.TISC	.G.SS..G..N.VS	WYQQ.PG.APKLLIY	....RPS	GVPDRFSGSKSGT.ASLTISGLQ.EDEADYYC	V	FG.GTKLTVLG	
8C	IQMTQS.S.L.A.V.D.V..T.	RATQ.ISTH--LN-	....RG.K.......	GASTLE.	...S.....G...EFT....S..P..F.T...	LQHRSYPWT---	..Q..NVEIK-	V$_\kappa$1
12E	SYE....P.A..T....V....	S.S..SI.S-ET.N	....L..T......	SNNQ...	...............S...A......S...	TAWDDTLNGRVI	..G.........	V$_\lambda$1
26H	.TVV..EP.F.V...GTI.LT.	DLN.GLVSSSHYP.	....T..Q..RT...	NTNI.S.	...AIL.NK.A...T.A.A...S....	VLYMGSGIS--.	..G.........	V$_\lambda$8
27D	.SA....A.V......SI....	T.T..DL.GH.F..	....H..K....M..	DVFN...	..SS.....NT.........A......F.	SSYIITNIV--.	..R.........	V$_\lambda$2
80R	TTLTQS.ATL.L...E.A.L.	RASQ.VRSN--LA-	....K..Q..RP...	DAST.AT	.I......G...DFT....R.EP..F.V...	QQRSNWPPT---	..Q...VE.K-	V$_\kappa$3
91M	.SA.....A.V......SI....	T.T..DV.GY.F..	....H..K....M..	DVSK...	..............NT.........A......F.	SSYTITDIV--.	..G.........R	V$_\lambda$2
92N	.PG....P.A..T....V....	S.SR.NI.G-.T.N	...HV..T......	SNNQ...	...............S..A...RS....E...	ATWEDSLSGY-.	..P...V....	V$_\lambda$1

Framework regions 1–4 (FW1–4), and complementarity-determining regions 1–3 (CDR1–3) for both the VH and VL are shown. The VH and VL family designations are also shown. Consensus amino acids are shown if they are encoded by >50% of VH or VL genes at a given position. A dot in the consensus sequence is shown if ≤50% of genes encoded the same amino acid. Dots in individual sequences represent the same amino acid as the consensus. Dashes represent gaps.

human whole IgG1 (80R IgG1). Binding kinetic rates (K_{on} and K_{off}) and affinities of 80R scFv, 80R IgG1, and ACE2 receptor for S1-Ig were measured by surface plasmon resonance. As shown in Table 2, 80R IgG1 had a 20-fold increase ($K_d = 1.59$ nM) in binding affinity to S1 over its parental 80R scFv ($K_d =$

32.3 nM), which is comparable to that of the receptor ACE2 ($K_d = 1.70$ nM). In a further microneutralization assay, as shown in Fig. 1B, 80R IgG1 was 20-fold more effective than 80R scFv on a molar basis comparison, which was consistent with its superior affinity (Fig. 1B). At a concentration of 7.43 nM, 80R
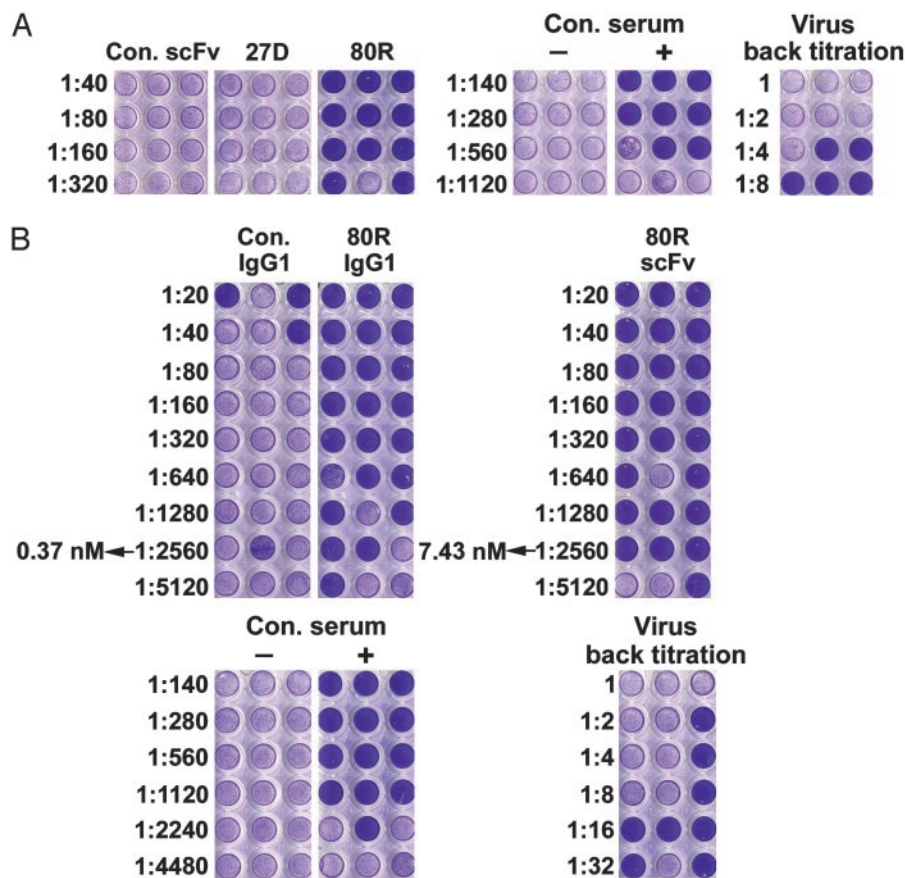

Fig. 1. Microneutralization assay of anti-S1 antibodies on SARS-CoV. (A) Microneutralization assay of anti-S1 scFvs. The positive control was convalescent serum from a SARS patient; the negative control was non-SARS human serum. The names of the scFvs are labeled at the top, and antibody titers are indicated on the left. Neutralizing scFv 80R and only one nonneutralizing scFv 27D (illustrative of the other nonneutralizing scFvs) are shown. Undiluted SARS-CoV (≈37 plaque-forming units) was loaded per well. (B) Comparison of the neutralization activity of 80R scFv and full-length 80R IgG1. The positive and negative control serum samples and the amount of virus used were the same as in A. The titer and concentration of antibodies are labeled on the left.

Table 2. Kinetic rates and binding affinity of 80R antibody and ACE2 to S1-Ig

	K_{on}, M^{-1}·s^{-1}	K_{off}, s^{-1}	K_a, M^{-1}	K_d, M
80R scFv	2.29×10^5	8.36×10^{-3}	3.10×10^7	3.23×10^{-8}
80R IgG1	3.88×10^5	6.18×10^{-4}	6.28×10^8	1.59×10^{-9}
ACE2	2.47×10^5	4.20×10^{-4}	5.88×10^8	1.70×10^{-9}

Kinetic rates and K_a and K_d were calculated using BIA-EVALUATION software.

scFv can neutralize >50% of the testing wells from infection, whereas the same neutralizing activity was achieved by 80R IgG1 at a concentration as low as 0.37 nM.

Inhibition of Syncytia Formation and Binding of S1 to ACE2 by 80R. Because SARS-CoV S protein-expressing 293T cells can fuse with receptor ACE2-expressing 293T cells to form multinucleated syncytia, we performed a syncytia formation inhibition assay with all eight anti-S1 scFvs and 80R IgG1. Consistent with the neutralization results, 80R was the only scFv that inhibited syncytia formation (data not shown). 80R IgG1 was also more potent in blocking syncytia formation than 80R scFv, as shown in Fig. 2. These results indicated that the mechanism by which 80R neutralized SARS-CoV could be direct inhibition of virus attachment to cell membrane through blocking binding of S1 to ACE2. To confirm this directly, we first examined whether the 80R scFv could inhibit the binding of S1 to ACE2-expressing Vero E6 cells. As shown in Fig. 3A, when Vero E6 cells were

incubated with S1-Ig in the presence of 80R scFv and analyzed by flow cytometry, 80R scFv completely inhibited the binding of S1-Ig to Vero E6 cells at a concentration of 15 μg/ml (about five times greater molar concentration than S1-Ig), whereas a non-neutralizing antibody 27D did not inhibit the binding under the same conditions. S1 (327)-Ig, which is not part of the receptor-binding domain (15), was used as a control for S1-Ig-specific binding to Vero E6 cells. Second, the binding of S1-Ig to metabolically labeled soluble ACE2 was specifically inhibited by 80R scFv in a dose-dependent manner (Fig. 3B). Collectively, these data demonstrate that the primary mechanism of the neutralizing activity of 80R is through blocking of S1 binding to ACE2.

Characterization of 80R Epitope. Primary characterization of 80R epitope showed that 80R recognized SDS-denatured, DTT-reduced, and PNGase F-deglycosylated S1 in an immunoblotting assay (Fig. 4A), although binding is greater under nonreduced conditions. This suggests that the 80R epitope is more sensitive to reduction, more resistant to denaturation, and independent of glycosylation. Mapping of the 80R epitope showed that it was located within the N-terminal 261–672 amino acids of S protein, as shown in Fig. 4B, 80R did not recognize the S1 (327)-Ig but recognized the S1 (261–672)-Ig as determined by Western blotting. This is of interest when compared to the neutralizing epitopes on S protein of murine hepatitis virus (MHV), which have been mapped to the N-terminal 330 amino acids of S1 (20). Although MHV is thought to be a closest relative of SARS-CoV, the SARS-CoV is only distantly related to any of the three known
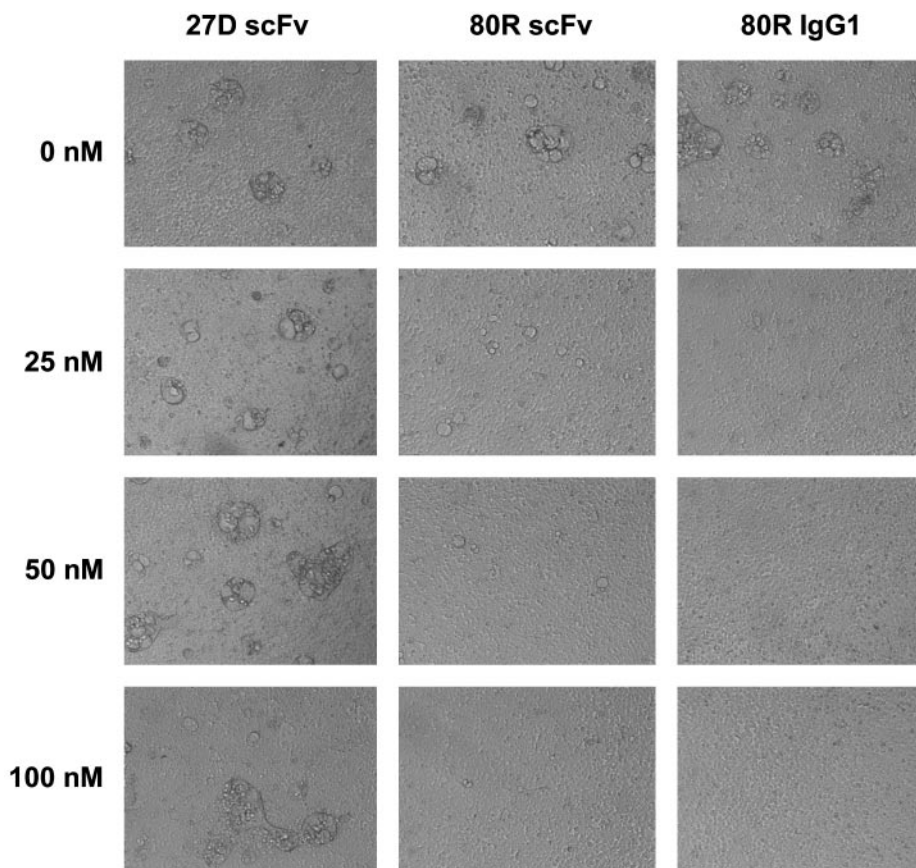

Fig. 2. Inhibition of syncytia formation by anti-S1 antibodies. Shown is syncytia formation assay with anti-S1 antibodies. 293T cells expressing SARS-CoV S protein were preincubated with the indicated concentrations of anti-S1 scFvs or 80R IgG1 and then mixed with 293T cells expressing ACE2. After culturing for 36 h in the presence of antibodies, dose-dependent inhibition of syncytia formation by 80R scFv, 80R IgG1 was observed and photographed. Representative results are shown.
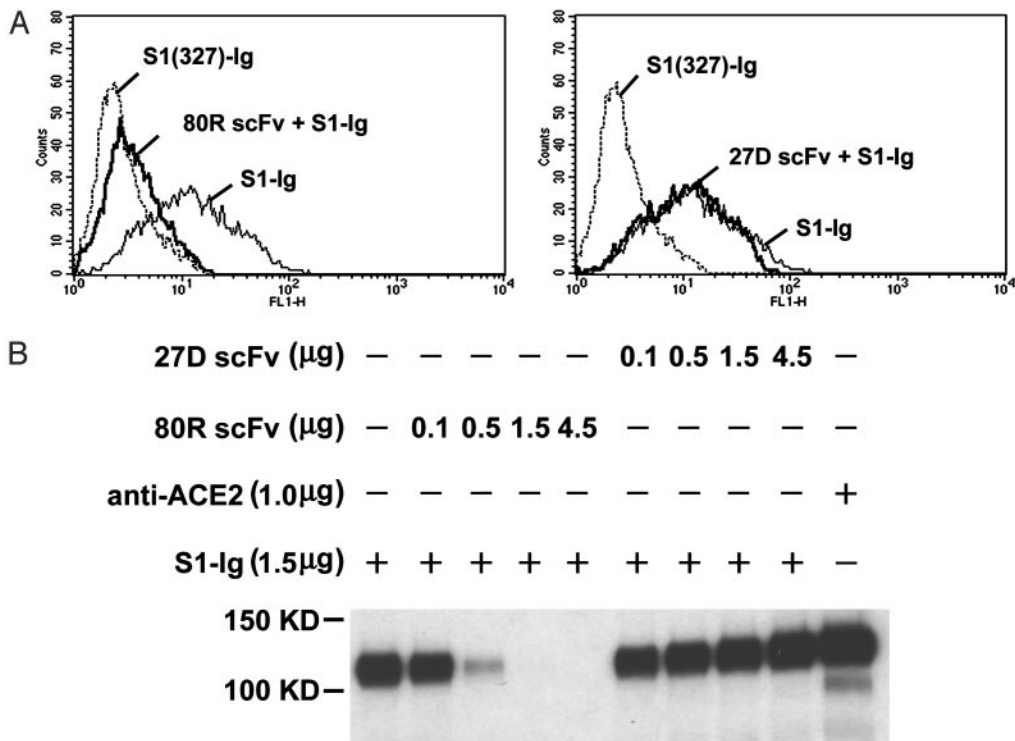
Fig. 3. 80R scFv inhibiting the binding of S1 to ACE2 receptor. (*A*) Flow cytometry histograms; shown is staining Vero E6 with S1-Ig and flow cytometry analysis. Dotted line, control staining with S1 (327)-Ig; thin line, cells were stained with S1-Ig; bold line, staining with premix of 0.3 µg of S1-Ig and 0.3 µg of 80R scFv (*Left*) or 27D scFv (*Right*). (*B*) scFv competition of S1-Ig binding to ACE2 in immunoprecipitation. Radiolabeled ACE2 was immunoprecipitated by S1-Ig that was preincubated with the indicated amounts of either 27D scFv or 80R scFv. Anti-ACE2 precipitates were used as a positive control. Immunoprecipitates were run on a reducing SDS/PAGE gel and visualized by autoradiography.

classes of coronavirus and has now been assigned to a fourth group (7–8). The sequence similarity of S protein of SARS-CoV and the S protein of MHV is low (26.5% pairwise amino acid identity), and the functional receptor for the SARS-CoV is ACE2, which is quite different from the receptor of MHV (BGP,

Fig. 4. Western blotting of S1-Ig using 80R scFv. Nonreduced, reduced, or deglycosylated samples were subjected to 10% SDS/PAGE gel, transferred to nitrocellulose membrane, detected with anti-S1 80R scFv, and followed by rabbit anti-His-6 Ig and horseradish peroxidase-labeled anti-rabbit IgG. (*A*) 80R scFv recognized nonreduced S1 much stronger than reduced S1, and there is no further significant decrease of antibody binding to deglycosylated S1 as compared with reduced S1. (*B*) 80R scFv bound to S1 (261–672)-Ig but did not bind to S1 (327)-Ig. All samples were run under reducing conditions.

a member of the carcinoembryonic antigen family of the Ig superfamily) (8, 15, 21). Therefore, it is not surprising that the receptor-binding domain and the neutralizing epitopes on these two viruses are localized to different regions on S protein. Further work will be required to define the precise structure of the 80R epitope, which will likely have important implications for anti-SARS drug development and the design of vaccines capable of eliciting a protective 80R-like antibody response.
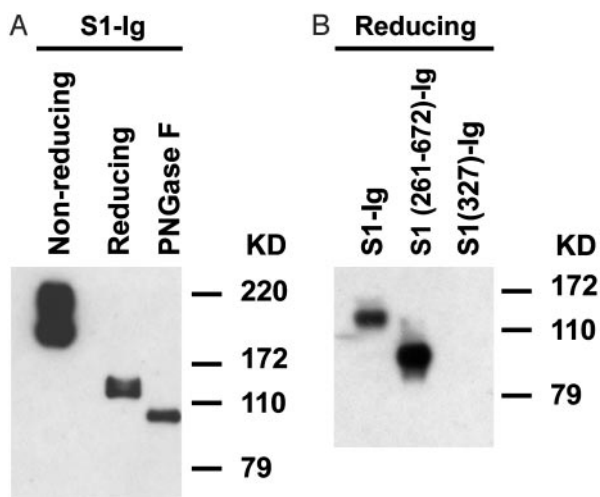
Conclusion

In summary, we have identified an anti-S1 human monoclonal antibody 80R with a nanomolar affinity that potently neutralizes SARS-CoV infection and efficiently inhibits syncytia formation through blocking of receptor binding. The approach used in our investigation is noteworthy in that a potent neutralizing high-affinity antibody against an emerging pathogen was readily selected from nonimmune human antibody library. Passive immunization has been proven to be an effective and safe strategy for the prevention and treatment of viral disease (22–25). The passive administration of neutralizing human monoclonal antibodies could provide an immediate treatment strategy for emergency prophylaxis and treatment of SARS, while the alternative and more time-consuming development of vaccines and new drugs is underway. Although *in vivo* antiviral activities of 80R remain to be investigated in the clinical setting, good correlation between the antibody-neutralizing activity *in vitro* and the protection *in vivo* for many different viruses, challenge routes, and animal models has been reported (26–27). Our *in vitro* data suggest that the 80R human monoclonal antibody can be further developed and tested in *in vivo* animal studies to determine its clinical utility as a potent viral entry inhibitor for emergency prophylaxis and treatment of SARS.

1. Ksiazek, T. G., Erdman, D., Goldsmith, C. S., Zaki, S. R., Peret, T., Emery, S., Tong, S., Urbani, C., Comer, J. A., Lim, W., *et al.* (2003) *N. Engl. J. Med.* **348,** 1953–1966.
2. Kuiken, T., Fouchier, R. A., Schutten, M., Rimmelzwaan, G. F., van Amerongen, G., van Riel, D., Laman, J. D., de Jong, T., van Doornum, G., Lim, W., *et al.* (2003) *Lancet* **362,** 263–270.
3. Drosten, C., Gunther, S., Preiser, W., van der Werf, S., Brodt, H.-R., Becker, S., Rabenau, H., Panning, M., Kolesnikova, L., Fouchier, R. A. M., *et al.* (2003) *N. Engl. J. Med.* **348,** 1967–1976.
4. Holmes, K. V. (2003) *N. Engl. J. Med.* **348,** 1948–1951.
5. Pearson, H., Clarke, T., Abbott, A., Knight, J. & Cyranoski, D. (2003) *Nature* **424,** 121–126.
6. Li, G., Chen, X. & Xu, A. (2003) *N. Engl. J. Med.* **349,** 508–509.
7. Holmes, K. V. (2003) *J. Clin. Invest.* **111,** 1605–1609.
8. Rota, P. A., Oberste, M. S., Monroe, S. S., Nix, W. A., Campagnoli, R., Icenogle, J. P., Penaranda, S., Bankamp, B., Maher, K., Chen, M.-h., *et al.* (2003) *Science* **300,** 1394–1399.
9. Gallagher, T. M. & Buchmeier, M. J. (2001) *Virology* **279,** 371–374.
10. Spiga, O., Bernini, A., Ciutti, A., Chiellini, S., Menciassi, N., Finetti, F., Causarono, V., Anselmi, F., Prischi, F. & Niccolai, N. (2003) *Biochem. Biophys. Res. Commun.* **310,** 78–83.
11. Moore, K. M., Jackwood, M. W. & Hilt, D. A. (1997) *Arch. Virol.* **142,** 2249–2256.
12. Daniel, C., Lacroix, M. & Talbot, P. J. (1994) *Virology* **202,** 540–549.
13. Koo, M., Bendahmane, M., Lettieri, G. A., Paoletti, A. D., Lane, T. E., Fitchen, J. H., Buchmeier, M. J. & Beachy, R. N. (1999) *Proc. Natl. Acad. Sci. USA* **96,** 7774–7779.
14. Song, C., Lee, Y., Lee, C., Sung, H., Kim, J., Mo, I., Izumiya, Y., Jang, H. & Mikami, T. (1998) *J. Gen. Virol.* **79,** 719–723.
15. Li, W., Moore, M. J., Vasilieva, N., Sui, J., Wong, S. K., Berne, M. A., Somasundaran, M., Sullivan, J. L., Luzuriaga, K., Greenough, T. C., *et al.* (2003) *Nature* **426,** 450–454.
16. Harrison, J. L., Williams, S. C., Winter, G. & Nissim, A. (1996) *Methods Enzymol.* **267,** 83–109.
17. Schier, R., Marks, J. D., Wolf, E. J., Apell, G., Wong, C., McCartney, J. E., Bookman, M. A., Huston, J. S., Houston, L. L. & Weiner, L. M. (1995) *Immunotechnology* **1,** 73–81.
18. Bai, J., Sui, J., Zhu, R. Y., Tallarico, A. S., Gennari, F., Zhang, D. & Marasco W. A. (2003) *J. Biol. Chem.* **278,** 1433–1442.
19. Reff, M. E., Carner, K., Chambers, K. S., Chinn, P. C., Leonard, J. E., Raab, R., Newman, R. A., Hanna, N. & Anderson, D. R. (1994) *Blood* **83,** 435–445.
20. Kubo, H., Yamada, Y. K. & Taguchi, F. (1994) *J. Virol.* **68,** 5403–5410.
21. Williams, R. K., Jiang, G. & Holmes, K. V. (1991) *Proc. Natl. Acad. Sci. USA* **88,** 5533–5536.
22. Keller, M. A. & Stiehm, E. R. (2000) *Clin. Microbiol. Rev.* **13,** 602–614.
23. Casadevall, A. (2002) *Nat. Biotechnol.* **20,** 114.
24. Shibata R, Igarashi, T., Haigwood, N., Buckler-White, A., Ogert, R., Ross, W., Willey, R., Cho, M. W. & Martin, M. A. (1999) *Nat. Med.* **5,** 204–210.
25. Igarashi, T., Brown, C. Azadegan, A., Haigwood, N., Dimitrov, D., Martin, M. A. & Shibata, R. (1999) *Nat. Med.* **5,** 211–216.
26. Burton, D. R. (2002) *Nat. Rev. Immunol.* **2,** 706–713.
27. Parren, P. W. & Burton, D. R. (2001) *Adv. Immunol.* **77,** 195–262.

MICROBIOLOGY